

Characterization of (4,4)- and (5,3)-type Stacking-faults in 4deg.-off 4H-SiC Epitaxial Wafers by Synchrotron X-ray Topography and by Photo-Luminescence Spectroscopy.

T. Yamashita^{1,2,a*}, H. Matsuhata^{1,3}, Y. Miyasaka^{1,2}, M. Odawara^{1,2},
K. Momose^{1,2}, T. Sato^{1,2,b}, and M. Kitabatake¹

¹R&D Partnership for Future Power Electronics Technology (FUPET) , 2-9-5 Toranomon, Minato-ku,Tokyo 105-0001, Japan

²SHOWA DENKO K.K., 1-13-9, Shibadaimon, Minato-ku,Tokyo 105-8518, Japan

³Advanced Power Electronics Research Center, National Institute of Advanced Industrial Science and Technology, 1-1-1, Umezono, Tsukuba, Ibaragi 305-8568, Japan

^at-yamashita@fupet.or.jp, ^bTakayuki_Sato@sdk.co.jp

Keywords: Silicon carbide (SiC); Stacking-Faults; Partial dislocation; Synchrotron X-ray Topography; Photo-Luminescence Spectroscopy

Abstract. Experimentally, the grazing-incident X-ray topography at different diffraction conditions, and room temperature photo-luminescence spectroscopy, various different types of stacking-faults in epitaxial films on 4-degrees-off 4H-SiC wafers were identified precisely without wafer cutting. Their types and the numbers were investigated statistically. It became clear that (4,4) type stacking-faults were the most common ones and two different types were identified. Still 34% of the stacking-faults were unknown types in the present investigation.

Introduction

Current SiC wafers contain several types of defects in their epitaxial film. Among them, stacking-faults are one of the most common defects. It was reported that stacking-faults and poly-types with smaller band-gaps will impact negatively on SBD performances [1]. It was reported that some types of stacking-faults affected negatively carrier life times as well [2]. Also, it can be considered that different types of stacking-faults are generated by different causes. To improve the quality of epitaxial films, precise identifications of types of stacking-faults and statistical investigations of the faults will be necessary.

Photo-Luminescence (PL) imaging and spectroscopy is efficient for investigating locations of many different types of stacking-faults and to identify their types. However, emission peaks in PL spectrums for some types of stacking-faults are located at very close to each other and the peak sharpness is not enough to distinguish different types at room temperature. For precise identification, low-temperature PL or high-resolution electron microscopy has been used [3]. But those methods are neither efficient experimental, nor suitable for statistical investigations for whole surface of an epitaxial film since wafer cutting is necessary for those methods.

Stacking-faults that give emission peaks of PL spectrum at very close positions to each other have different types of partial dislocations along outlines of the faults, i.e. Shockley type and Frank type [3]. Their Burgers vectors directions are different, thus they can be distinguished by crystallographic method such as X-ray topography.

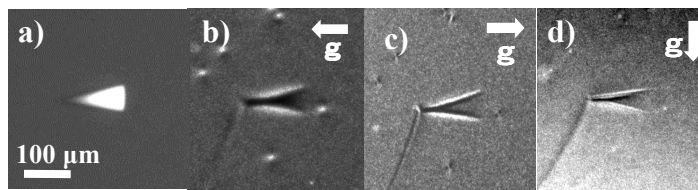
In this paper, we demonstrate one of our results on type distribution of triangular-shaped and bar-shaped stacking-faults observed in a 4-degrees-off 4H-SiC epitaxial wafer using Synchrotron X-ray Topography and room temperature PL Spectroscopy without wafer cutting. And the lattice displacements around (4,4)- and (5,3)-type of triangular shaped stacking-faults were discussed with observed results.

Experimentals

Commercially available 3 inch 4H-SiC wafers with $10\ \mu\text{m}$ -thick epitaxial films with 4-degrees off-cut from the $[0001]$ to the $[11\bar{2}0]$ direction, and with carrier concentration of $N_d=5\times 10^{14}/\text{cm}^3$ were used. PL colored imaging experiments were carried out to find the locations of stacking-faults in the epitaxial films and then experiments of PL imaging with band-pass filters were carried out to estimate emission wavelength of these stacking-faults. In both measurements, the 340 nm light of Hg-lamp was used as an excitation source. PL spectra excited by the 325nm light of He-Cd laser were also obtained. For identifications of stacking-faults by PL experiments the data by Ref. [3] and [4] were used. Grazing-incidence Bragg-case synchrotron reflection X-ray topography experiments were carried out at BL15C in Photon-Factory to observe partial-dislocations at the edge of stacking-faults. Reflections used for the analyses were $\mathbf{g}=\bar{1}\bar{1}28$, $11\bar{2}8$, $\bar{2}118$, $1\bar{2}18$, $\bar{1}018$, $0\bar{1}18$, and $1\bar{1}08$ at wavelength of 0.15 nm.

One example of identification result was shown in Fig. 1. This stacking-fault showed PL peak at around 480nm in Fig. 1 (a), indicating the possibilities of both Shockley (5,3)-type and Frank intrinsic type by Ref [3]. In the grazing incidence X-ray topographic image, clear asymmetric contrasts of partial dislocations at the outlines of the triangular shapes were observed in Fig. 1(b) for $\mathbf{g}=\bar{1}\bar{1}28$, (c) $\mathbf{g}=11\bar{2}8$ and (d) $\mathbf{g}=1\bar{1}08$. The asymmetric contrasts for partial dislocations were unchanged depending on reflections, indicating that these were partial dislocations with Burgers vectors not on the basal plane. Thus this stacking-fault was regarded as a Frank intrinsic type one.

Furthermore, triangular-shaped defects that showed emission of around 520nm or that showed no emission in PL measurements were not applicable because not stacking-fault but bulk 3C-type inclusions were thought to be formed.



Figs. 1 Frank-type stacking-fault.

These images are of the same scale.

a) PL image (480 nm filtered image).

b) Topographic image at $\mathbf{g}=\bar{1}\bar{1}28$ condition

c) Topographic image at $\mathbf{g}=11\bar{2}8$ condition

d) Topographic image at $\mathbf{g}=1\bar{1}08$ condition

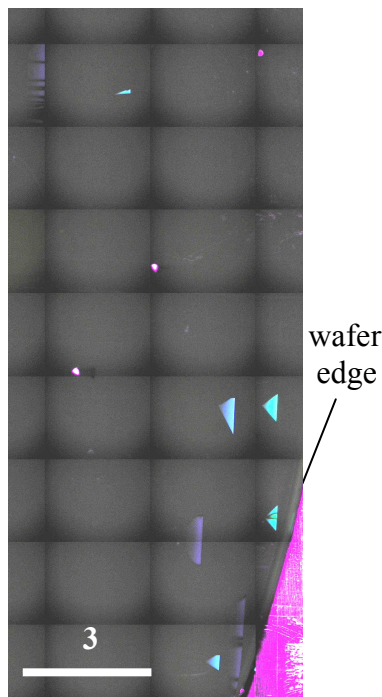


Fig. 2 A colored PL image of a wafer. Purple stick contrasts correspond to the Bar-Shaped defects.

Results and Discussions

Fig.2 shows an example of colored PL image of a wafer. Contrasts with wavelength of visible region were displayed with RGB device. Triangular shaped stacking-faults were shown according to their emission wavelength. 4H-SiC normal region that emitted a wavelength of 390nm were displayed as gray region. Several different types of stacking-faults were observed in the epitaxial film. According to an investigation of whole surface on a 3 inches wafer, 33 bar shaped defects and 30 triangular shaped stacking-faults were observed, for example.

Result of identification for triangular shaped stacking-faults for one wafer was shown in Fig. 3. 23% of triangular shaped were identified as Frank type and 43% were as Shockley type, and 3%, 27%, and 13% were identified as (1,3), (4,4), and (5,3) types, respectively [4]. The (6,2) type stacking-faults were not seen in this wafer. In the present experiment, 34% of triangular shaped stacking faults remained as unclear and un-identified types.

We need more detailed analysis to identify these unclear type of stacking-faults using other analysis method such as TEM observations, though this method is not efficient and not suitable for statistical analysis, but will be necessary for clear identifications. Though,

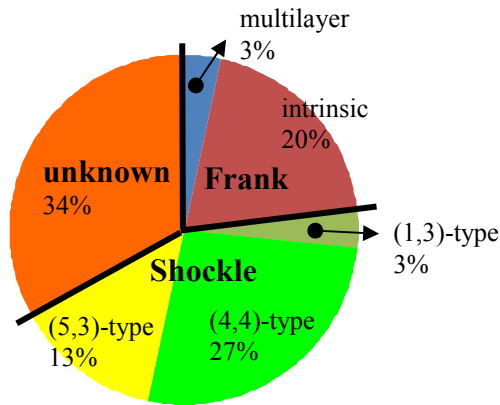


Fig. 3 Identification result of triangular-shaped stacking-faults in a wafer.

except those un-identified type, the stacking-faults on one epitaxial wafer could be identified easily with the present method.

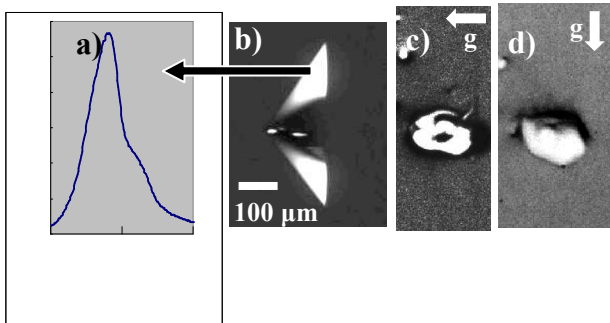
In the present analysis, two different types of stacking-faults for Shockley (4,4) type were identified. Figs.4 and Figs.5 show those two types of the X-ray topographic images of (4,4) stacking- faults.

-Type-I: No clear contrasts of the partial dislocations at the outlines of the triangular shapes were observed at all reflection conditions.

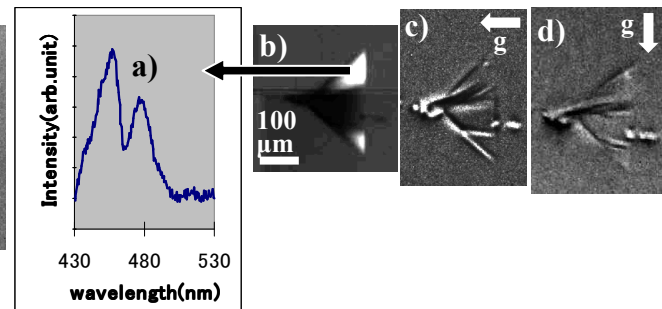
-Type-II: Clear contrasts of the partial dislocations at the edges of the triangular shapes were observed, and very clear reverses

of asymmetric contrast along partial dislocations were observed depending on sign of $\mathbf{g} \cdot \mathbf{b}$ for \mathbf{g} vectors used for observations, and \mathbf{b} vector for the partial dislocations as seen in Fig. 5.

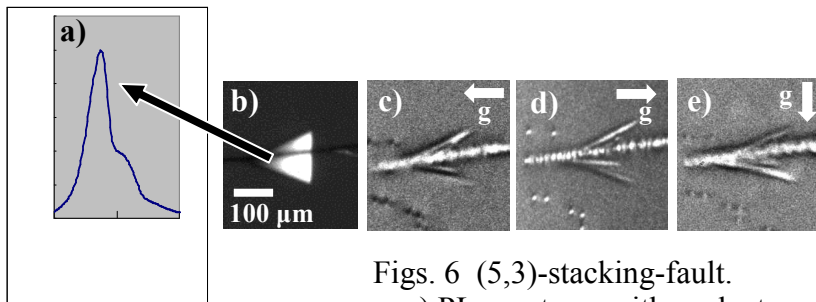
On the other hand, all of the observed X-ray topographic images for (5,3) stacking-faults gave clear asymmetric contrast at the edges of the triangular shapes, and the contrasts were changed depending on reflections, as shown in Fig.6, similar to the case for type-II (4,4). In Fig.4, 5 and 6, images were taken from same area. PL image b) and topographic images c), d) and e) have the same scale. Topographic images in Fig, c), d) and e) were taken under $\mathbf{g} = \bar{1}\bar{1}28$, $\mathbf{g} = 11\bar{2}8$, and $\mathbf{g} = 1\bar{1}08$ conditions, respectively.



Figs. 4 Type-I (4,4)-stacking-fault.
a) PL spectrum with peak at around 460nm
b) PL image (460 nm filtered image)
c) and d) Topographic images



Figs. 5 Type-II (4,4)-stacking-fault.
a) PL spectrum with peak at around 460nm
b) PL image (460 nm filtered image)
c) and d) Topographic images



Figs. 6 (5,3)-stacking-fault.
a) PL spectrum with peak at around 480nm
b) PL image (480 nm filtered image)
c), d) and e) Topographic image

These results were considered as the differences of Burgers vectors for Shockley partial dislocations formed at boundaries between stacking-faults and normal 4H structure regions. Boundaries of (4,4) stacking-faults consist of four Shockley-type partial dislocations [4]. At boundaries of (4,4) type-I in Fig.4, Burgers vectors of the partials 4 dislocations must have been cancelled out to reduce strain energy at the edge of the stacking-fault, thus the long range strain field could not be observed in the topographic images. On the other hand, in case of (4,4) type-II in Fig.5, Burgers vectors of four partial dislocations were not cancelled out, and then the long-range strain fields remained. In case of (5,3) stacking-faults, the boundaries consist of three Shockley partial dislocations[4]. Because of the odd number of the Shockley partial dislocations, Burgers vectors could not be cancelled out thoroughly, and long-range strain field remained.

Summaries

We have investigated stacking-faults on an epitaxial wafer statistically on the types and the numbers by performing experiments of the grazing-incident X-ray topography at different diffraction conditions, as well as the photo-luminescence spectroscopy at room temperature without wafer cutting. We still had some un-identified stacking-faults. The two different types of (4,4) type stacking-faults were identified.

Acknowledgments

Photon-Factory, in High Energy Accelerator Research Organization is acknowledged. This work is supported by Novel Semiconductor Power Electronics Project Realizing Low Carbon Emission Society by METI and NEDO in Japan.

References

- [1] S. Harada, Y. Namikawa, and R. Sugie, Mater. Sci. Forum Vols. 600-603(2009),963-966.
- [2] S. Maximenko, J.A. Freitas, P.B. Klein, A. Shrivastava, and T.S. Sudarshan, Appl. Phys. Lett. 94 (2009) 0902101.
- [3] I. Kamata, X. Zhang, and H. Tsuchida, Appl. Phys. Lett. 97 (2010) 172107.
- [4] G. Feng, J. Suda, and T. Kimoto, Physica B 404 (2009) 4745-4748.

Silicon Carbide and Related Materials 2012

10.4028/www.scientific.net/MSF.740-742

Characterization of (4,4)- and (5,3)-Type Stacking-Faults in 4deg.-Off 4H-SiC Epitaxial Wafers by Synchrotron X-Ray Topography and by Photo-Luminescence Spectroscopy

10.4028/www.scientific.net/MSF.740-742.585

DOI References

[2] S. Maximenko, J.A. Freitas, P.B. Klein, A. Shrivastava, and T.S. Sudarshan, Appl. Phys. Lett. 94 (2009) 0902101.

<http://dx.doi.org/10.1063/1.3089231>

[3] I. Kamata, X. Zhang, and H. Tsuchida, Appl. Phys. Lett. 97 (2010) 172107.

<http://dx.doi.org/10.1063/1.3499431>

[4] G. Feng, J. Suda, and T. Kimoto, Physica B 404 (2009) 4745-4748.

<http://dx.doi.org/10.1016/j.physb.2009.08.189>